

Design of a low-concentration roof-mounted solar thermal collector for industrial heat production

Cameron Stanley¹, David Ferrari¹, Leesa Blazley^{1,2}, Ahmad Mojiri^{1,3} and Gary Rosengarten¹

¹*RMIT University, School of Engineering, 115 Queensberry St, Carlton, VIC 3053, Australia*

²*BlueScope Steel, 120 Collins Street, Melbourne, VIC 3000, Australia*

³*Rheem, 1 Alan Street, Rydalmere NSW 2116, Australia*

E-mail: cameron.stanley@rmit.edu.au

Abstract

This paper presents the design of a roof-mounted solar thermal system consisting of a CPC collector and evacuated tube receivers which utilise thermal oil as the working fluid. The design process employed in this work considers the transmission and absorption of solar energy, optical losses due to the receiver-reflector gap, heat transfer within the receiver, and the thermal losses. Impacts of collector module tilt and CPC acceptance angle on annual energy gain were also included.

The collector system has a packaged height of 100mm, ensuring its appearance is similar to traditional flat-plate collectors when installed. The collector is intended to supply renewable process heat for applications with loads between 150°C-250°C, with a target thermal efficiency of 50% at 200°C. A prototype collector is currently in production and will be tested in the latter months of 2016 at the RMIT University solar test laboratory in Melbourne.

1. Introduction

Industrial process heat represents a considerable fraction of the total energy consumed within Australia [1]. Currently the overwhelming majority of this heat is generated via the combustion of natural gas, with a smaller contribution by electric resistance heating and heat pumps. In order to reduce fossil fuel consumption a renewable alternative for this process heat is highly desirable.

RMIT University, together with its partners, has been developing a roof-mounted solar collector as part of the Australian Renewable Energy Agency (ARENA) funded Micro Urban Solar Integrated Concentrators (MUSIC) project to address this requirement. The aim is to develop a low-concentration non-tracking solar thermal collector capable of producing 200°C heat suitable for supplying renewable heat for industrial processes.

Compound Parabolic Concentrators (CPCs) are low optical-concentration non-imaging solar collectors which are capable of concentrating solar radiation over a broad range of acceptance angles [2]. For this reason they lend themselves well to non-tracking, roof mounted applications for the generation of low-medium temperature thermal energy. Winston et al. [3] demonstrated the use of a CPC solar collector for generating the heat required to run a 23kW double effect absorption chiller. Their system was capable of producing 200°C at 40% efficiency, although had a profile height of approximately 270mm.

In an attempt to make a low-profile product more suited to inconspicuous roof mounting, one of the key objectives of the project was to ensure the collector height remains <100mm (arbitrary but mandated). This would ensure the aesthetics of the collector are not vastly different to typical PV panels, or existing flat-plate solar thermal collectors. Additionally it would help to reduce collector weight; a necessity for ensuring light weight support structures and low cost installation on industrial roof-tops.

2. Collectors Design

The collector design consists of two main components: a CPC to concentrate sunlight and an evacuated tube thermal absorber. The design of each of these components is strongly linked to the other. The method used to design the current collector is covered in the following sections. It should be noted that it is intended to incorporate a more thorough optimisation process for a second generation collector, as well as an investigation of the annualised performance evaluation using TRNSYS simulations.

2.1. Design Method

The following approach was employed for the design of the collector:

1. Acceptance angles chosen based on sun path for the given installation location and the minimum intended duration of light capture.
2. Collector tilt determined by optimization of energy capture over the year
3. Absorber size and CPC geometry determined by optical/thermal efficiency modeling
4. Steady-state performance predicted using analytical heat transfer model

The collector has been designed with a nominal operating temperature of 200°C and is intended for installation in Melbourne Australia, latitude - 37.8° S, longitude - 144.9° E, aligned in the East-West orientation. Irradiance data for this location has been taken from the Australian Solar Radiation Data Handbook, 4th Edition, 2006 [4].

2.2. CPC acceptance angle

The ideal concentration ratio of a CPC collector is given by $C = 1/\sin(\theta_A)$, where θ_A is the half-acceptance angle. The broader the intended acceptance window, the lower the concentration, and hence lower the possible collector temperatures.

In this case the acceptance angle for the CPC was determined by the intended length of heat production throughout the year. The collector was to be able to capture the sun at its peak in summer, and provide a minimum generation of 2hrs on the shortest day of the year. As such, the upper limit for the elevation angle to be accepted by the CPC is defined by the highest solar elevation at the summer solstice, 75.6°. Whereas, the minimum elevation angle for which the collector will accept sunlight was set at 27°. An additional 3° angle was applied to each of these limits to allow for the high reflection losses which result at the edge of the acceptance window [5]. Figure 1 shows the range of sun elevation angles which are within this acceptance window through the year in Melbourne.

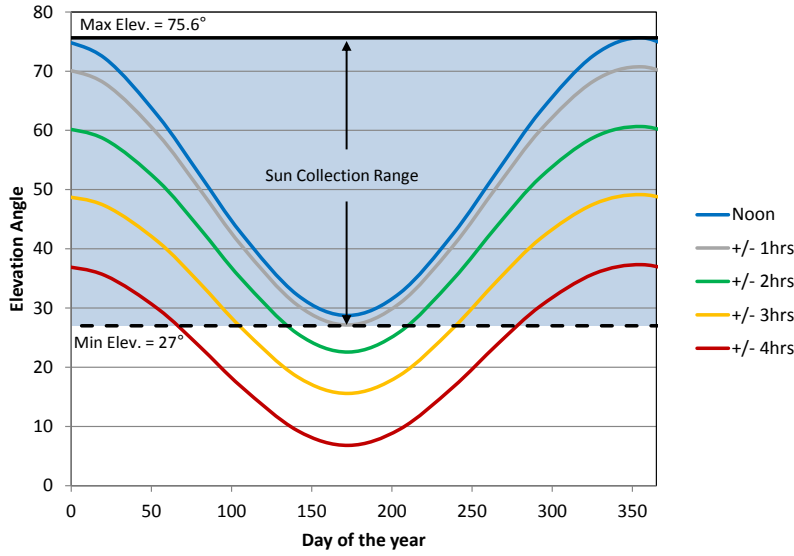


Figure 1. Sun elevation angle for Melbourne showing the acceptance band for this CPC collector.

2.3. Collector tilt

Optimal collector module tilt angle was determined by optimising the energy capture of the collector over the year. Representative days for each month were used to determine the anticipated collection duration.

The global irradiance on a module plane tilted at angle β can be expressed as

$$S_{\text{mod}} = S_{\text{in}} [\cos(\alpha) \sin(\beta) \cos(\psi - \theta) + \sin(\alpha) \cos(\beta)] \quad (1)$$

where S_{in} is the total irradiance on a sun tracking plane, α is the sun elevation angle, θ is the sun azimuth angle, and ψ is the azimuth angle to which the collector faces ($\psi = 0^\circ$ for north facing). Elevation angle is expressed as

$$\alpha = \sin^{-1} [\sin(\delta) \sin(\psi) + \cos(\delta) \cos(\psi) \cos(\text{HRA})] \quad (2)$$

where HRA is the hour angle and δ is the sun declination angle, expressed as a function of the day of the year, d , as

$$\delta = \sin^{-1} [\sin(23.45^\circ) \sin(360/365(d - 81))]. \quad (3)$$

The optimal collector tilt was obtained by maximising the annual energy yield from the collector, as follows

$$E_{\text{yr}}(\beta) = \max_{0 < \beta < 90} \sum_{\text{month}=1}^{12} \sum_{\text{HRA}=-75}^{75} \frac{I_{g,\text{max}} S_{\text{mod}}}{S_{\text{in}}} \eta_{\text{th}}(I_g) dt \quad (4)$$

where $I_{g,\text{max}}$ is the maximum average global intensity for each month and $\eta_{\text{th}}(I_g)$ is an expression for collector efficiency as a function of global intensity. The summation is performed with hour angle resolution of 1° over the 12 representative days of the year. The resultant optimal collector tilt is $\beta = 36.92^\circ$, which is just less than the latitude angle of the installation, a result of imposing a minimum elevation acceptance angle of 27° . It should be

noted that this choice was arbitrary and chosen as much for potential marketing value (year-round solar generation) as for engineering reasoning. A true optimisation approach here would be iterative, allowing both the minimum elevation angle and the collector tilt to be determined by the energy yield rather than be imposed based on minimum sun collection duration in winter. This adaption has been adopted for work currently underway for a second generation collector.

2.4. CPC Geometry

With the acceptance angle and collector tilt determined the CPC geometry was then determined using the method presented by Sin Kim et al. [6]. It can be quickly seen that the normal to the collector aperture is aligned at an angle of $\gamma = (90 - \beta) = 53.08^\circ$. This does not bisect the upper and lower limit of elevation angles presented in section 2.2, requiring different half-acceptance angles on the northern and southern sides of the CPC to fully capture the sunlight over the year. For ease of manufacturing a symmetrical half-acceptance angle has been adopted which is the arithmetic mean of the two. The symmetric CPC is then rotated about the absorber to ensure that alignment of the acceptance window with respect to the collector aperture is maintained. This introduces an optical axis tilt of $\theta_t = 1.77^\circ$.

In order to define the CPC geometry the receiver diameter and gap between the bottom of the receiver and the cusp of the mirror are required. In order to arrive at the optimal configuration the optical and thermal performance of the CPC and absorber need to be modelled. This process simulates the absorption of solar radiation on the receiver, transfer of heat to the working fluid and all heat losses from the system to determine the overall optical and thermal efficiency. Details of this process are presented in section 0.

Whilst the design intention was to minimize the gap losses of the receiver there is a lower limit governed by practicality, as this gap needs to be sufficiently large that manufacturing tolerances and droop due to thermal expansion and the weight of the heat transfer fluid do not cause the thermal absorber tube to come into contact with the borosilicate glass tube. This gap also includes the thickness of the glass tube itself.

A final absorber diameter of $d_i = 16$ mm was selected, with a gap of $g = 4.5$ mm. Once these parameters are chosen the CPC curves were generated. The final rotated CPC was then unevenly truncated to ensure the packed height of the whole collector remains equal to 85mm, allowing a further 15mm to accommodate any required stiffening ribs, framing or enclosure beneath the mirror surface.

To meet the requirement for the whole collector to be no more than 100mm in height the CPC was then unevenly truncated such that the height between the lowest point on the northern side of the collector and the aperture plane was 85mm (15mm allowance for CPC substrate material and supports etc.). The geometry of the resultant CPC, together with a summary of the important parameters is shown in Figure 2. Figure 3 shows the orientation of the CPC collector with respect to a horizontal plane and the minimum acceptance angles of the sun.

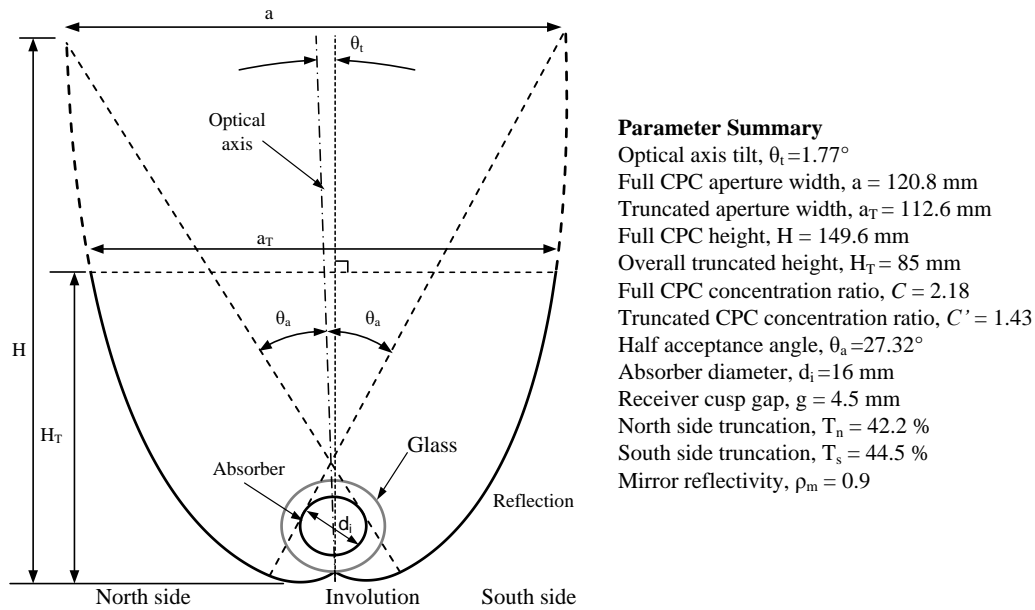


Figure 2. Geometry of symmetric CPC, rotated and asymmetrically truncated.

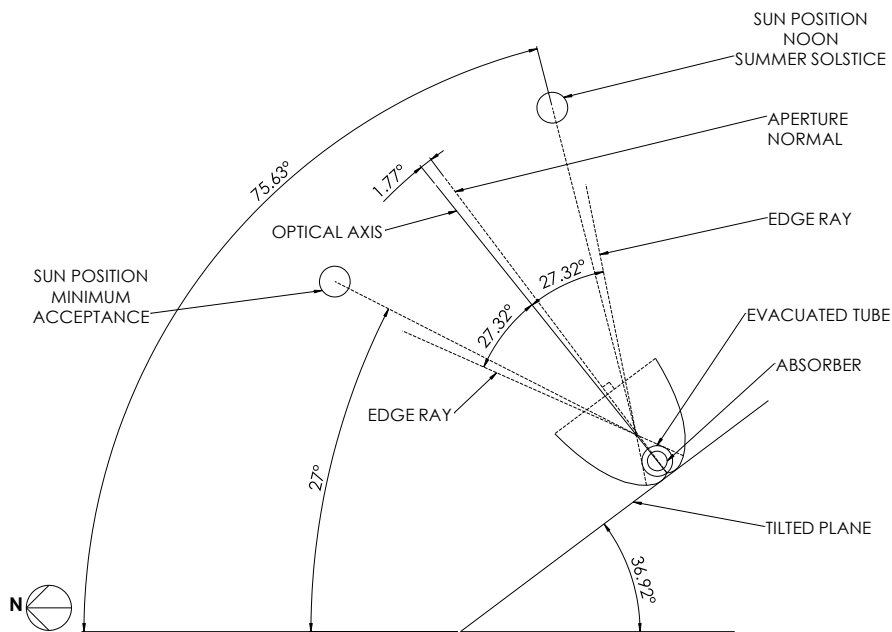


Figure 3. Geometry of symmetric CPC, asymmetrically truncated – View facing East.

Various methods for fabricating the CPC were investigated including injection moulding, fiberglass lay-up and vacuum forming. A full discussion of manufacturing methods along with their associated geometrical tolerances and the influence these have on the optical performance of the CPC are presented in a separate paper.

Overall length of the mirror was capped at 1m – a decision to limit the collector to a unit size which could allow single person installation.

2.5. Evacuated absorber tubes

The evacuated tube thermal absorbers for this collector were produced by Greenland Systems Solar, an Australian solar thermal company with manufacturing capabilities in China.

Originally a u-bend style thermal absorber was designed, following on from the work of Karwa et al. [7]. However, in the interest of achieving a tangible outcome for this project a number of technical concessions were made. Discussions with Greenland Systems and their manufacturing team in China eliminated both the u-bend and counter flow annular receivers due to the complexity of achieving the manufacturing tolerances required. Ultimately, a flow through receiver design was adopted in which the fluid passes through a single tube which serves as the thermal absorber. A schematic of the evacuated absorber is shown in Figure 4.

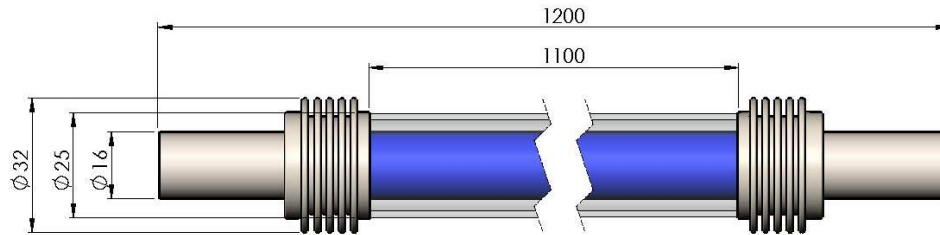


Figure 4. Evacuated absorber tube dimensions

The absorbers tubes are surrounded by a borosilicate glass tube, which is evacuated via a fusible hole in the glass. Kovar bellows at each end of the absorber accommodate differential thermal expansion between the absorber and the glass tube. A summary of the evacuated tube dimensions and thermal properties are presented in Table 1.

Table 1. Evacuated absorber tube properties

Component	Property	Symbol	Value	Unit
Glass	Material	-	Borosilicate	-
	Length	L	1,100	mm
	Outer Diameter	D_g	25	mm
	Thickness	t_g	1.5	mm
	Reflectivity	ρ_g	0.07	-
	Absorptivity	α_g	0.01	-
	Emissivity	ε_g	0.915	-
Absorber	Length	L	1,100	mm
	Outer Diameter	d_o	16	mm
	Wall thickness	t_a	1.2	mm
	Absorptivity – short λ	$\alpha_{a,solar}$	0.974	-
	Absorptivity – long λ	$\alpha_{a,IR}$	0.07	-
	Emissivity	ε_a	0.112*	-
	Material	-	Stainless Steel	-
	Thermal conductivity	k_a	17	W/mK

$$* \varepsilon_a @ 200^\circ\text{C} - \varepsilon_a(T) = 2.73 \cdot 10^{-7} T^2 + 1.74 \cdot 10^{-4} T + 0.0664$$

3. Thermal Modelling

The thermal modelling conducted within this work is an extension of the modelling conducted by Karwa et al. [7]. As such, the reader is directed there for a full description of the

mathematics. The methods developed by Karwa have been employed here to arrive at the final design prototype. For brevity, only pertinent modelling information is presented here.

Modelling is conducted in the following five sections:

1. Absorption of solar radiation.

The solar irradiance absorbed by the evacuated tube and the receiver is calculated based on the total solar radiation energy reaching the aperture, the optical transmission of the CPC mirror (a function of the average number of reflections), the relative transmission, reflection and absorption characteristics of the evacuated tube and absorber. Diffuse and reflected radiation terms are considered to be isotropic and are modelled using view factors.

2. Thermohydraulics of the receiver.

The heat gained by the fluid within the absorber is determined via consideration of the flow regime within the tube and the total thermal resistance between the fluid and the receiver outer wall. The Nusselt number for all flow regimes are estimated using the correlations of Gnielinski [8]. Consideration is also given to the hydraulic power required to pump the fluid.

3. Thermal losses from the receiver and evacuated tube.

The thermal loss from the receiver is determined by analysis of the thermal energy exchange between the receiver and the evacuated tube, and between the evacuated tube and the sky. Experimentally measured, temperature dependent, emissivity of the TiNOX solar selective coating has been used.

4. Energy balance:

The equations derived for the solar energy absorption and thermal losses were used to formulate steady-state energy balance equations for the receiver and evacuated tube as

$$Q_r - Q_u - Q_{r-e} = 0, \quad (5)$$

$$Q_e + Q_{r-e} - Q_{e-\infty} = 0. \quad (6)$$

Here Q_r and Q_e are the solar energy absorbed by the receiver and evacuated tube respectively, Q_u is the useful heat gained by the fluid, Q_{r-e} is the radiation exchange between the receiver and the evacuated tube, and $Q_{e-\infty}$ is the exchange of energy (radiation and convection) between the evacuated tube and the ambient.

These two non-linear equations were then solved simultaneously within MATLAB to determine the receiver and evacuated tube temperature. The solution residuals are typically of the order of 10^{-6} when converged. The solution was iterated using temperature dependent thermophysical properties until the receiver and evacuated tube temperatures converged to within 0.001%.

5. Performance evaluation:

The collector optical and thermal efficiency were then calculated. The optical efficiency is defined as

$$\eta_{op} = \frac{Q_r}{Q_a} \quad (7)$$

where Q_r is the solar energy absorbed on the surface of the receiver. Q_a is the total solar radiation;

$$Q_a = (I_b + I_d)A_a \quad (8)$$

where I_b and I_d are the beam and diffuse component of solar radiation and A_a is the collector aperture area. The absorber tube thermal efficiency is defined as

$$\eta_{th} = \frac{Q_u}{Q_a} \quad (9)$$

Incorporating header tube heat losses, pumping power and accounting for the total energy resources required to obtain the thermal energy gain, an effective thermal efficiency can be defined as

$$\eta_{eff} = \frac{Q_{total}}{P_{total}} = \frac{Q_u + P_{hyd} - Q_h}{Q_a + P_t} \quad (10)$$

Here P_{hyd} is the hydraulic power required to pump the fluid through the collector (converted to heat via friction) and Q_h is the heat lost from the collector header and fluid connections. P_t is the thermal equivalent of the mechanical pumping power

$$P_t = \frac{P_{hyd}}{\eta_{pump}\eta_{GTD}}, \quad (11)$$

and includes the pump efficiency, η_{pump} , taken to be 0.7 (includes hydraulic, mechanical and electrical efficiency) and an electricity generation, transmission and distribution efficiency, η_{GTD} , taken to be 0.33.

3.1. Assumptions

The following assumptions are made for the analysis:

1. The ideal concentration ratio for the full (un-truncated) CPC is given by $C = 1/\sin(\theta_A)$, where θ_A is the half-acceptance angle. A geometric concentration ratio is defined based on the receiver and aperture areas as $C' = A_a/A_r$.
2. Any beam radiation incident upon the aperture within the acceptance angle will be reflected by the mirrored surface of the CPC onto the receiver and the gap. The fraction of diffuse radiation entering the aperture that will reach the receiver is given by the view factor from the aperture to the receiver, as per Rabl et al. [9].
3. The optical properties of the mirror, receiver and evacuated tube are assumed to be independent of incident angle.
4. For simplicity, the thermal resistance of the evacuated tube is neglected, as modelling showed the temperature difference from inside to outside $< 1K$ over a range of modelled parameters.

- End-effects, due to a finite length absorber and non-normal angle of incidence in the longitudinal plane have not been considered.

4. Modelled Performance

Figure 5 shows the effective thermal efficiency, η_{eff} , plotted against mean collector temperature, T_m , for irradiance of $I_g = 1000 \text{ W/m}^2\text{K}$ ($I_b = 850 \text{ W/m}^2\text{K}$, $I_d = 150 \text{ W/m}^2\text{K}$). Results are plotted for both aluminium and silver mirrors, with reflectivity of $\rho_m = 0.9$ and $\rho_m = 0.97$ respectively. At the nominal design condition of 200°C the effective thermal and optical efficiency is predicted to be $\eta_{eff} = 50.0\%$ and $\eta_{op} = 71.5\%$ for the aluminium mirror and, $\eta_{eff} = 56.4\%$ and $\eta_{op} = 78.0\%$ for the silver mirrors. Under these conditions the heat loss in the manifold, Q_h , represents 13.8% and 12.4% of the total useful heat collection, $Q_u + P_{hyd}$, for the aluminium and silver mirrors respectively. These results indicate the importance of the reflectivity of the CPC mirror coating on the collector performance. Currently a collector prototype is being constructed which will be used to experimentally validate this model and allow annualised simulations using transient energy simulation software TRNSYS.

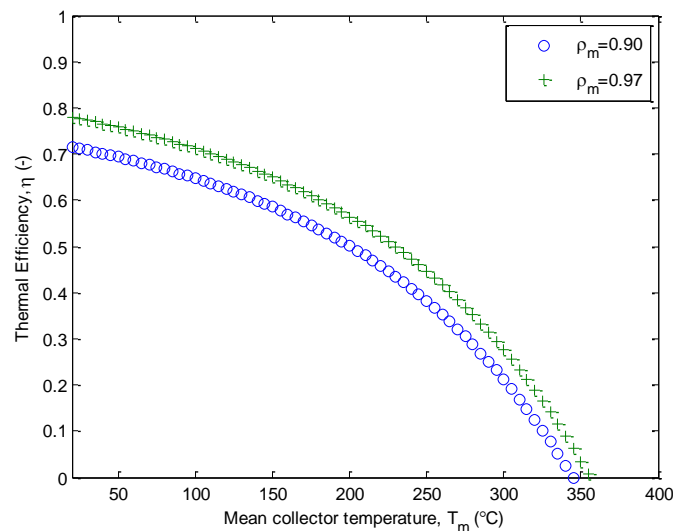


Figure 5. Modelled effective thermal efficiency.

5. CPC collector Prototype

A CAD representation of prototype currently being tested at RMIT is shown in Figure 6. The collector consists of 8 parallel tubes connected via two stainless steel fluid manifolds. For clarity the manifold insulation is not shown. The prototype CPC is constructed from a single piece of RenShape 460 styling board from which the CPC geometry was machined using a CNC router. The mirror coating was then applied to this piece via sputtering of aluminium, which is then coated with a protective layer of silicon dioxide. The mirror was measured to have an AM1.5 weighted reflectance of $\rho_m \approx 0.9$. Figure 7 shows some images of the evacuated tube receivers, the manifold assembly and the aluminium sputtered CPC.

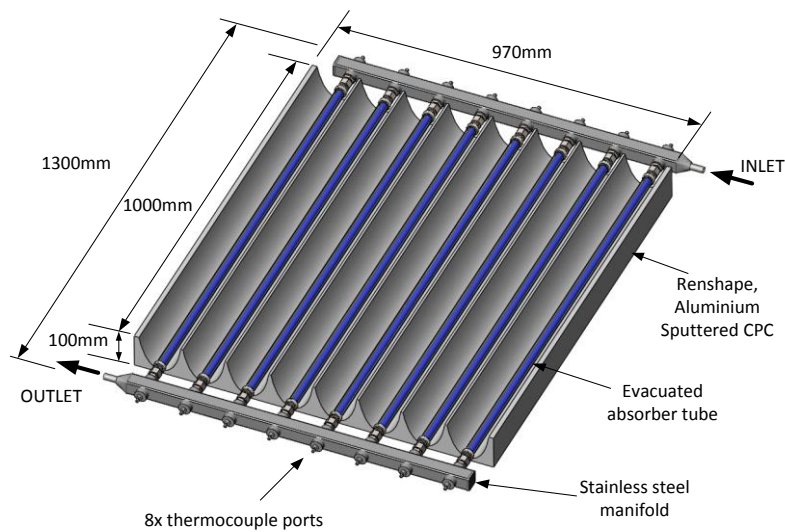


Figure 6. CAD representation of the collector prototype being tested at RMIT.

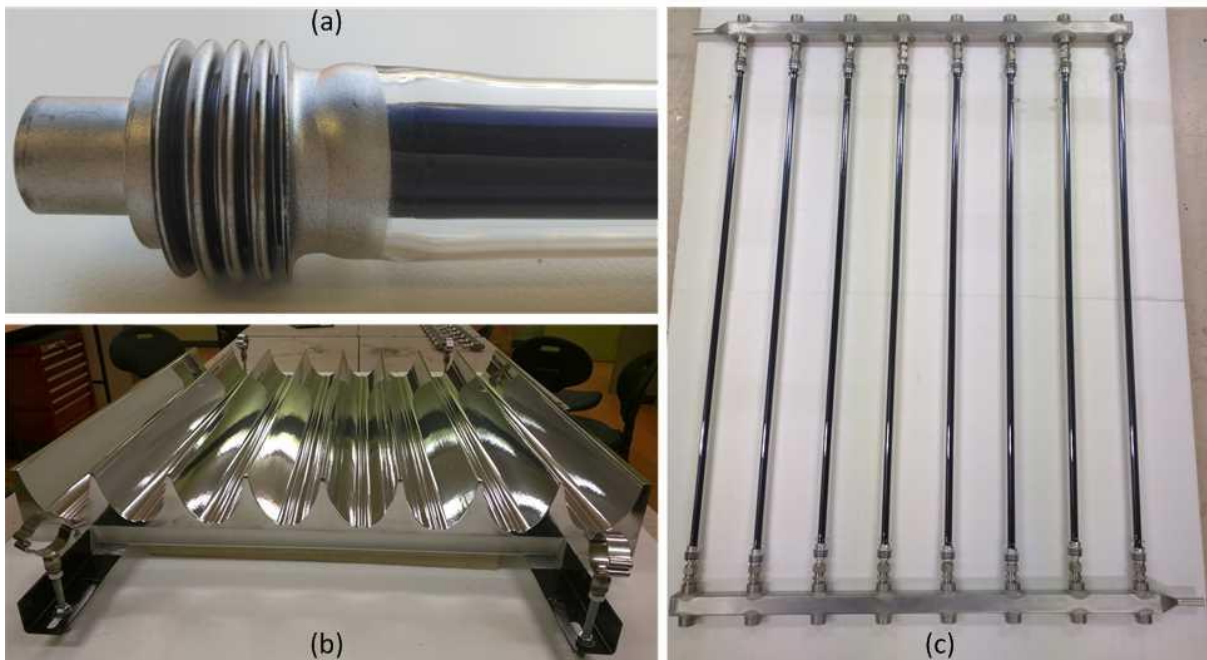


Figure 7. Prototype Collector: (a) close up of evacuated tube bellows, (b) aluminium sputtered RenShape CPC, and (c) absorber tube and manifold assembly.

Conclusions

This paper presents the design and development of a low-concentration non-tracking solar thermal collector for the production of industrial heat. A symmetric CPC, rotated about the optical axis by 1.77° has been used to provide year-round energy production in Melbourne. Uneven truncation of the two sides of the CPC allow the total collector height to remain under 100mm. A thermal model of the collector demonstrated an effective thermal efficiency of 50% was possible when the CPC mirror is produced from sputtered aluminium. A prototype is currently under construction and will be tested in the coming months at the RMIT solar laboratory in Melbourne.

References

1. Lovegrove, K., et al., *Renewable Energy Options for Australian Industrial Gas Users*, 2015, ARENA, prepared by: IT Power, Turner, ACT.
2. Winston, R., *Principles of solar concentrators of a novel design*. *Solar Energy*, 1974. **16**(2): p. 89-95.
3. Winston, R., et al., *Performance of a 23KW solar thermal cooling system employing a double effect absorption chiller and thermodynamically efficient non-tracking concentrators*. *Energy Procedia*, 2014. **48**: p. 1036-1046.
4. *Australian Solar Radiation Data Handbook*. 4th ed. 2006, Sydney: Australian and New Zealand Solar Energy Society.
5. Gajic, M., et al., *Modeling reflection loss from an evacuated tube inside a compound parabolic concentrator with a cylindrical receiver*. *Optics express*, 2015. **23**(11): p. A493-A501.
6. Kim, Y.S., et al., *Efficient stationary solar thermal collector systems operating at a medium-temperature range*. *Applied Energy*, 2013. **111**: p. 1071-1079.
7. Karwa, N., et al., *Receiver shape optimization for maximizing medium temperature CPC collector efficiency*. *Solar Energy*, 2015. **122**: p. 529-546.
8. Gnielinski, V., *G1 Heat Transfer in Pipe Flow*, in *VDI Heat Atlas*. 2010, Springer Berlin Heidelberg. p. 691-700.
9. Rabl, A., et al., *Practical design considerations for CPC solar collectors*. *Solar Energy*, 1979. **22**(4): p. 373-381.

Acknowledgements

The authors would like to acknowledge the work of Dr Nitin Karwa in the development of the thermal model used within this work. We also wish to acknowledge ARENA for providing the funding for this research via the MUSIC project.